International Journal of Science and Research (IJSR)
ISSN (Online): 2319-7064, Impact Factor (2013): 4.438
www.ijsr.net

The Effect of Mg Substitution on Structural and Dielectric Behiviour of Srcozn Mixed Nano Hexaferrites

Dilip Badwaik[a], Vandana Badwaik[2], Halim Ahamad[3], Shesh Chopne[4]

[1]Kamla Nehru Mahavidyalaya, Nagpur. (India) 440009

[2]Nutan Bharat College, Nagpur.(India) 440010

[3]S.F.S. College, Seminari Hills, Nagpur.(Nagpur)

[4]D. B. Science College, Gondia. (India)

Abstract: ***A series of polycrystalline $Sr_2Co_{1-X}ZnMg_XFe_{12}O_{22}$ Y-type nano hexaferrites substituted with magnesium; (x = 0, 0.1, 0.2, 0.3, 0.4) were synthesized by microwave assisted auto combustion method. Structural characterizations of the samples have been done using X-ray powder diffraction pattern. The prepared samples are in single Y –type hexagonal phase with the space group $R\bar{3}m(no.166)$. The lattice parameters, experimental density, X-ray density and porosities of samples were measured from XRD data. It is observed that the lattice parameter "a" is almost remains constant and easy magnetized "c" axis undergoes contraction with content of Mg. The crystallite size in the range 38- 72 nm is calculated from the XRD data. The ac electrical conductivity, dielectric constant and dielectric loss are measured in the range 100Hz to 0.2MHz. It was found that, the ac conductivity shows dispersion at high frequencies. This dispersion was explained on the basis of interfacial polarization that formed due to the inhomogeneous structure of ferrite material.***

Keywords: Y-type nano hexaferrites, XRD, AC electrical conductivity, Dielectric constant,

1. Introduction

Polycrystalline hexaferrites are good magnetic semiconductor with low electrical conductivity and low eddy current. They play a very important role in various technological applications such as microwave devices, high speed recording media, ferrofluids, catalysis and magnetic refrigeration systems [1]. The electrical and dielectric properties of the hexaferrites can be tailored to specific device applications by choice of different cations and cation distribution between interstitial sites. Method of preparation, sintering temperature, sintering time and preparation condition are also important parameters that affect properties of hexaferrites [2]. The magnetic properties of hexaferrites [3], d c electrical conductivity and thermoelectric power of Y-type hexaferrites [4], the dielectric properties and ac conductivity of W-type and M- type [5, 6] have been extensively studied. The ac conductivity of ferrites gives valuable information related to the localization of charge carriers at grain, grain boundaries, inter-granular tunneling of charge carriers across the grain boundary and dielectric polarization of magnetic ions [7,8].

The crystal structure of Y-type hexaferrites consist of basic units of hexagonal M ferrite and cubic spinel ferrites that retain a hexagonal crystal structure usually with direction of magnetization parallel to c- axis. Y-type hexaferrites consider as interesting and promising high frequency material, because of their very usefulness in VHF and UHF.

In the present paper, we synthesized Y- type nanohexaferrites with generic formula $Sr_2Co_{1-X}ZnMg_XFe_{12}O_{22}$ (where x = 0, 0.1, 0.2, 0.3, 0.4) by microwave assisted auto combustion route from metal nitrates and urea as a precursor. The synthesized samples where characterized by XRD, a c electrical conductivity (σ), dielectric constant (ε') and dielectric tangent loss (tanδ).

2. Experimental Procedure

2.1 Synthesis Technique

Magnesium substituted SrCoZn Y ferrite having generic formula $Sr_2Co_{1-X}ZnMg_XFe_{12}O_{22}$ (where x = 0, 0.1, 0.2, 0.3, 0.4) were prepared by microwave assisted auto combustion method .The starting chemicals used were AR grade Strontium nitrate, Cobalt nitrate, Zinc nitrate, Iron nitrate, Magnesium nitrate, and urea. Stoichiometric amount of all metal nitrates were put in a 500 ml borosil beaker containing 30 ml amount of triple filter distilled water to prepare a solution, to which urea was added. The solution was stirred for 30 minutes then heated with continuous stirring at about 90 ^oC to obtained gel. The beaker containing gel was kept in a domestic microwave oven, and was irradiated with microwaves. Within 4 minutes of irradiation, dark brown fumes started coming out from the exhaust., immediately after that gel solution get fired and resulted into a foamy dark brown powder. The synthesized powder was grounded in a pestle mortar for about one hour, the powder then calcinated at 900 ^oC for about six hour in furnace. The furnace is then cooled to the room temperature by a natural way. The calcinated powders were again grounded to get fine powder of nano hexaferrites.

2.2 Preparation of Pellet

To make pallets few drop of polyvinyl acetate as a binder was added to the prepared powder and was pressed in form

Licensed Under Creative Commons Attribution CC BY

of pellets using dye punch of 10mm diameter and by applying a pressure of 6 tons. The binder was burnt off by heating pellets at 400°C for 2 hours. For dielectric measurements, the silver coating was applied on both sides of the pellet and cured for 10 minutes at 125 °C to have good contact of silver with ferrite sample.

2.3 Sample Characterizations

The structure was determined through the X-ray diffraction (XRD) analysis. XRD patterns were taken using Cu Kα (λ = 1.5406 Å) radiation at room temperature. The average crystallite size, lattice parameters, bulk density, X-ray density and porosity were calculated using simple formulae [9]. The dielectric measurements were carried out at room temperature in the frequency range 100 Hz – 0.2MHz using LCR-bridge (Model Hemeg- 8118).

3. Results and Discussions:

3.1 Structural Properties:

The X-ray diffraction patterns of $Sr_2Co_{1-X}ZnMg_XFe_{12}O_{22}$ (X= 0.0, 0.1, 0.2, 0.3, 0.4) Y- type hexaferrites samples obtained at room temperature along with a standard pattern are shown in Fig 1. All the XRD reflection peaks are indexed by applying a hexagonal crystal system. It is observed that most of the peaks of prepared sample are matched with standard pattern, reveals that they are Y–type hexagonal ferrite with the space group $R\bar{3}m(no.166)$.

The value of lattice parameter a, c, and their ratio c/a and unit cell volume V are summarized in Table1. It is observed that the lattice parameter 'a' is almost remains constant and easy magnetized 'c' axis undergoes more contraction with content of Mg. It follows the fact that all hexagonal ferrites exhibit constant lattice parameter 'a' and variable parameter 'c'. The variation in lattice constants with substitution indicates that substitutions are achieved on crystallographic sites. The decrease in the lattice parameter 'c' can be explained on the basis of the ionic radii. The ionic radii of the Mg^{+2} ion is (0.66 Å) and Co^{+2} ion is (0.72 Å). Since the ionic radius of Mg^{+2} is less than that of Co^{2+}, the decrease in lattice parameters with Mg^{+2} substitution is expected. It is shown that the value of the lattice parameter is in satisfactory agreement with the published results for Y- type hexagonal ferrite[10.11]. Table 1 show that theoretical variation of cell volume is in accordance with the experimental variation in bulk density.

The variation of experimental density D (Bulk density), X-ray density Dx (Theoretical density) and porosity P as a function as magnesium content is shown in Fig 2. It was found that the Dx values are

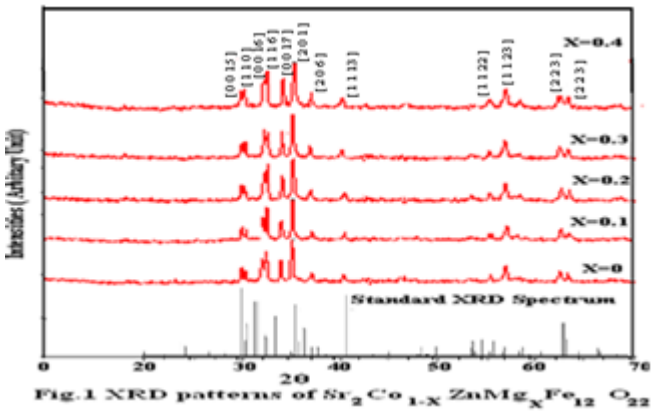

Fig.1 XRD patterns of $Sr_2Co_{1-X}ZnMg_XFe_{12}O_{22}$

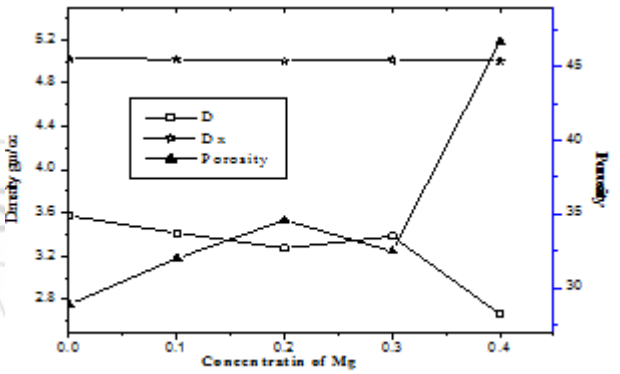

Fig.2 Variation of Dx, D and Porosity with con. of Mg

nearly same for all composition and close to 5.05 gm/cm^3 which are in agreement with the published results[12]. The experimental density values were found to be in general less than that X-ray density which was expected due to the presence of unavoidable pores created during sintering process. It is observed that the experimental density is slightly decreased with increase of Mg content, but the porosity is increased. This behavior may be attributed to the facts that introduction of Mg ions in hexagonal ferrite may affect the grain size development during sintering and increase porosity.

The XRD pattern is also used to calculate the grain size of the prepared compound. Grain size of all the compound are calculated from most intense peak using Scherer formula

$D=0.9\lambda/\beta\cos\theta$

Where λ is the wavelength.
β is the full width at half maxima (FWHM).
θ is the corresponding position at particular angle.
The crystallite size calculated is found to be in range of 38 nm to 72 nm.

3. 2 Frequency Dependence

The frequency dependent ac conductivity (log σ_{ac}); dielectric constant (ε') and dielectric loss (tan δ) were measured in the range 100 Hz – 0.2 MHz at room temperature for all prepared samples. Fig. 3 depicts ac conductivity as a function of frequency (log ω) for all samples. In general the results show dispersion in ac conductivity with respect to frequency. At relatively lower frequencies, the conductivity is increase slowly, but at relatively higher frequencies, conductivity begins to increase sharply. The dispersion of ac conductivity was observed before for other ferrites[13,14]. The dispersion in the ac electrical conductivity of polycrystalline

Licensed Under Creative Commons Attribution CC BY

ferrites is explained on the basis of interfacial polarization that formed due to the inhomogeneous structure of ferrite material. According to Maxwell and Wagner model and Koops phenomenological theory[15], the ferrite is imagined to act as a multilayer capacitor in which the ferrite samples are characterized by a microstructure consisting of conductive thick layers, grains (with conductivity σ_1; dielectric constant ε_1; and thickness d_1) separated by resistive thin layers, grain boundaries (with σ_2; ε_2; and d_2). The impedance of this multilayer capacitor can be represented as[16].

$$Z^{-1} = R^{-1} + J\omega c \quad (1)$$

Where ω is the angular frequency (ω= 2πf), R and *c* are the parallel equivalent resistance and capacitance of the material, respectively. According to Eq. (1), it is shown that above a certain frequency, the inverse impedance of the multilayer condenser and hence the ac conductivity of ferrite material rises with frequency.

The effect of frequency on the dielectric constant ε' is depicted in Fig. 4. It is shown that at relatively low frequencies the values of ε' is high and it decreases rapidly with increasing frequency.

Table 1: Lattice constants, cell volume, bulk density, crystallite size

Sr. No.	Content of Mg (X)	Lattice Parameter		Ratio c/a	Cell Volume $(Å)^3$	Bulk density gm/cc	Crystallite Size (nm)
		a (Å)	c (Å)				
1	0.0	5.874	44.93	7.648	1342.56	3.5752	72
2	0.1	5.878	44.90	7.638	1343.49	3.4145	53
3	0.2	5.870	44.85	7.640	1338.34	3.2751	53
4	0.3	5.873	44.78	7.624	1337.62	3.3839	38
5	0.4	5.876	44.73	7.610	1337.49	2.6662	42

The behavior of ε' with frequency can be explained on the basis of the assumption that the mechanism of the polarization process in ferrites is similar to that of the conduction process[17]. It is known that, in the case of zinc containing ferrite a partial reduction of Fe^{3+} ions to Fe^{2+} ion can take place as a result of volatilization of zinc during the sintering process[18]. It was suggested that, for cobalt containing ferrite, Co^{3+} ions can be formed during the sintering process due to reduction tendency of $Co^{2+} \leftrightarrow Co^{3+}$ and presence of Co^{2+} on the octahedral site favors the following exchange interaction

$$\mathbf{Co^{2+} + Fe^{3+} \leftrightarrow Co^{3+} + Fe^{2+}} \quad (2)$$

Thus the conduction mechanism for the samples under investigation can be explained with the aid of Verwey mechanism[19] and Heiks model[20], by two exchange interactions: electron hopping between Fe^{2+} and Fe^{3+} and hole transfer between Co^{3+} and Co^{2+} over the octahedral sites. The first exchange give rise to the displacement of the local charges in the direction of the external field leading to the main source of polarization in these ferrites, while the latter exchange gives rise to displacement of the holes in opposite direction of the external field leading to the second source of polarization in these ferrites. The decrease of the dielectric constant ε' with increasing frequency can be attributed to the fact that the electron exchange interaction between ferrous and ferric ions and hole exchange between Co^{3+} and Co^{2+} cannot follow the frequency of the external alternating electric field beyond a certain frequency value[21]. The high values of the dielectric constant of these ferrites at relatively low frequencies) can be attributed to the inhomogeneous structure of these ferrites[15].

Fig.5 shows the dielectric loss tangent behavior as a function of frequency for all samples. The loss tangent is defined as the ratio of the loss or resistive current to the charging current in the sample. Also it is known that, there is a strong correlation between the conduction mechanism and the dielectric constant behavior (the polarization mechanism) in ferrites. From these two considerations we can see that the behavior of tan δ with frequency is showing the expected decrease of tan *δ* with increasing frequency. The decrease of tan δ with f could be accounted for using Koops's model.

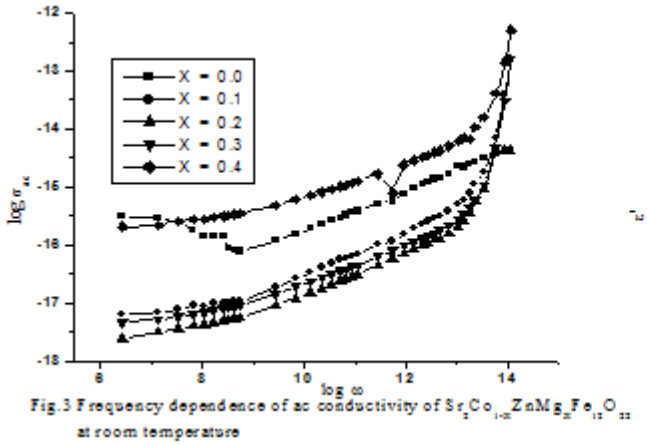

Fig.3 Frequency dependence of ac conductivity of $Sr_2Co_{1-x}ZnMg_xFe_{12}O_{22}$ at room temperature

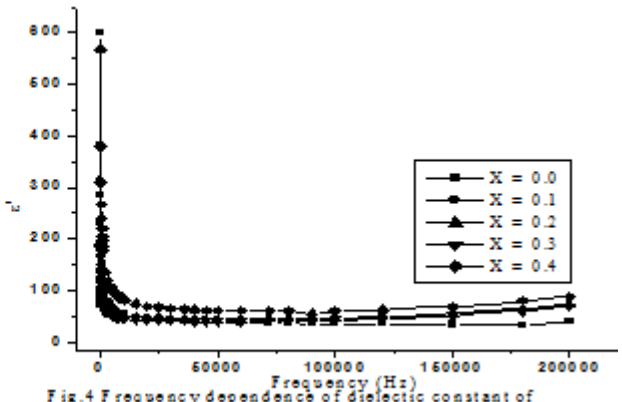

Fig.4 Frequency dependence of dielectric constant of $Sr_2Co_{1-x}ZnMg_xFe_{12}O_{22}$ at room temperature

In the low frequency region which corresponds to high resistivity (due to grain boundaries) more energy is required for electron exchange between Fe^{2+} and Fe^{3+} ions. Thus the energy loss is high. In the high frequency range which corresponds to low resistivity (due to the grains) a small energy is needed for electron transfer between Fe^{2+} and Fe^{3+} ions in the grains and hence the energy loss is small. The low loss values at higher frequencies show the potential

Licensed Under Creative Commons Attribution CC BY

applications of these materials in high frequency microwave devices[22].

3.4.3 The Composition Dependence:

The room temperature compositional dependence of the ac electrical conductivity (σ_{ac}), the dielectric constant (ε') and dielectric loss (tan δ) at 10kHz, 15kHz, 20kHz and 10k are illustrated in Fig. 6 to Fig. 8 respectively. It is shown that all the parameters decreases with increase in "x" until they reach a minimum value at X=0.2, after which they start to increase with further increase in Magnesium content. It stated that, the electric conduction in the studied sample is related mainly to the presence of the impurities and the hopping of charge carriers[4]. Since the number of the impurity atom is very limited, the hopping conduction mechanism plays a major role in the electric conduction and dielectric polarization process in these ferrites by electron hopping between Fe^{2+} and Fe^{3+} ions. It is well known that Mg^{2+} cations are distributed over all cations positions leading to mixed occupancies of positions in cation sublattice[23], while the iron ions are distributed between both A and B sites. The Co^{+2} ion generally preferred octahedral sites, but when particles size reduced to nanodimensions, there is change in cations distribution and Co^{2+} occupy both octahedral (B) and tetrahedral (A) sites[24]. Therefore the behavior of σ_{ac}, ε' and tan δ with composition can be explained as follows: The addition of Mg^{+2} ions up to concentration X=0.2 reduces the Co content at B sites which will reduce the probability of hopping given by

$$Co^{2+} + Fe^{3+} \leftrightarrow Co^{3+} + Fe^{2+}$$

Therefore conductivity decreases up to X=0.2. However beyond X=0.2 replacement of Co^{2+} ions by Mg^{2+} ions will force some of the iron ions to migrate from A-sites to B-sites to substitute the decrease in B-sites population[25]. Therefore the number of Fe^{2+} and Co^{3+} will increase accordingly to above equation. So, the hopping conduction by the electron transfer between Fe^{2+} and Fe^{3+} and holes transfer between Co^{2+} and Co^{3+} will increase. Consequently the electrical conductivity σ_{ac} increases. The behavior of ε' and tanδ can be explained on the basis of the assumption that the mechanism of dielectric polarization is similar to that of electrical conduction hence it is expected that behavior of ε' and tanδ is similar to that of σ_{ac}

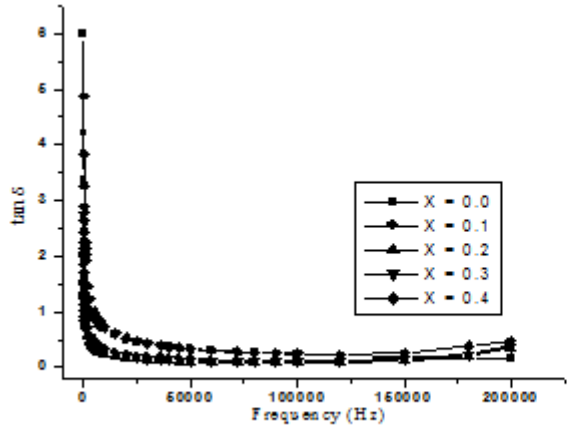

Fig.5 Frequency dependence of dielectric loss of $Sr_2Co_{1-X}ZnMg_XFe_{12}O_{22}$ at room temperature

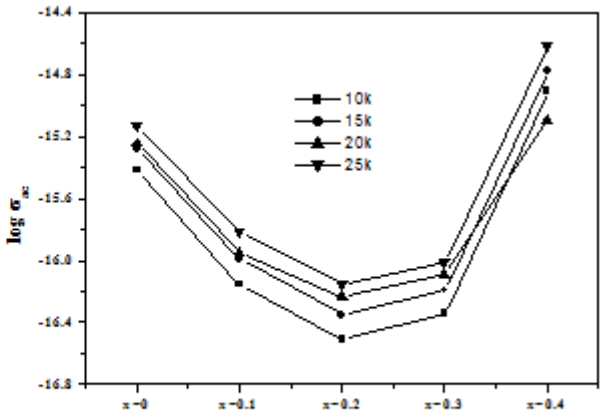

Fig. 6 Composition dependance of ac conductivity

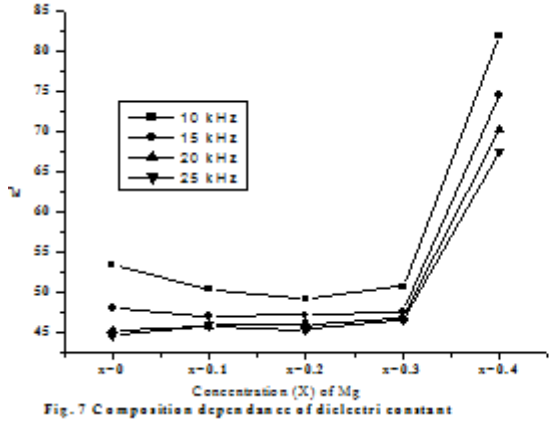

Fig. 7 Composition dependance of dielectri constant

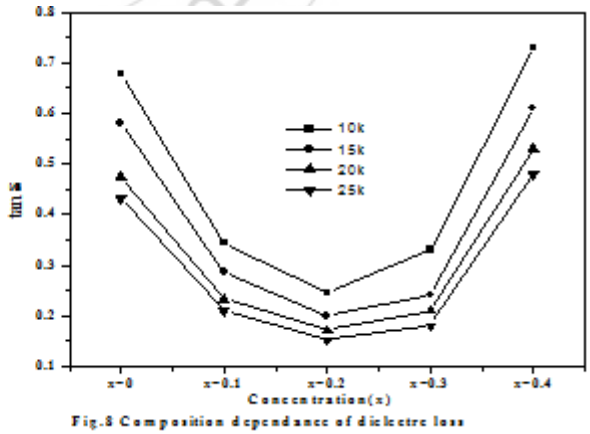

Fig.8 Composition dependance of dielectric loss

4. Conclusions

The X-ray diffraction patterns of $Sr_2Co_{1-X}ZnMg_XFe_{12}O_{22}$ (X= 0.0, 0.1, 0.2, 0.3, 0.4) Y- type hexaferrites samples confirm the formation of Y- type hexaferrites. It is observed that the lattice parameter 'a' is almost remains constant and easy magnetized 'c' axis undergoes more contraction with content of Mg. The decrease in the lattice parameter 'c' can be explained on the basis of the ionic radii. The ionic radii of the Mg^{+2} ion is (0.66 Å) and Co^{+2} ion is (0.72 Å). Since the ionic radius of Mg^{+2} is less than that of Co^{2+}, the decrease in lattice parameters with Mg^{+2} substitution is expected. The crystallite size is in the range 38- 72 nm. The dispersion of ac electrical conductivity was observed at higher frequencies. This dispersion was explained on the basis of

Licensed Under Creative Commons Attribution CC BY

interfacial polarization that formed due to the inhomogeneous structure of ferrite material.

References

[1] M. I Rosales., A. M Plata., M. E Nicho. , A.Brito, M.A.Ponce. V.M.Castano, J. Mater. Sci. **1995**, 30, 4446-4450
[2] M. Guyot, J. Magn. Magn. Mater. **1990**, 18, 925.
[3] H.J.Kwon, J. Appl. Phys. **1994**, 75(10), 6109.
[4] M.A. El Hiti, A.M.Abo, El Ata, J. Magn. Magn. Mater. **1999**, 195, 667
[5] D.EI Kony, S.A., Saafan, A,M Abo, EI Ata, Egypt. J. Sol., **2000** , 23 (1), 137-146
[6] A,M,Abo, EI Ata, M.A EI Hiti, J. Phys. III France **1997,** 7, 883.
[7] M. George, S.S. Nair, A.M. John, P.A. Joy, M.R. Anantharaman., J. Phys. D:Appl. phys.**2006,** 39, 900.
[8] I.H. Gul, A.Z. Abbasi, F. Amin, M.A. Rehman, A. Maqsood., J. Magn. Magn. Mater. **2007**, 311: 494.
[9] S. O. Kasap, 2006 Principles of electronic materials and devices (New York: McGram- Hill)
[10] Sajal Chandra Mazumdar, A. K. M. Akther Hossain, World Jour of Condensed Matter Physics,2 (2012) 181-87
[11] Vandana Badwaik, Dilip Badwaik, Vivek Nanoti, Kishor Rewatkar, International Jour of Knowledge Engg., Vol 3, Issue 1 (2012) 58-60
[12] Asmat Elahi, Mukhtar Ahmad, Ihsan Ali, M. U. Rana, Ceramics International, 39 (2013) 983-90
[13] M. Guyot, J. Magn. Magn. Mater. 15–18 (1980) 825
[14] B.K. Kuanr, G.P. Srivastava, P. Kishan, Proceedings of the ICF-5, 1989, India, p. 227.
[15] C.G. Koops, Phys. Rev. 83 (1) (1951) 121.
[16] S.A. Mazen, H.M. Zaki, J. Phys. D: Appl. Phys. 28 (1995) 1.
[17] K. Iwavchi, J. Appl. Phys. 10 (1971) 1520.
[18] C. Prakash, J.S. Baijal, J. Less-Common Met107 (1985) 51.
[19] E.J.W. Verwey, J.H. de Boer, J. Less Common Met. 106(1985) 257.
[20] R.R. Heikes, W.D. Johnston, J. Chem. Phys. 26 (1957) 582.
[21] V.R.K. Moorthy, J. Sobhamadri, Phys. Stat. Sol. A 36(1976) 133.
[22] K. M. Batoo and M.S. Ansari, Nanoscale Res. Lett. 7 (2012) 112-125
[23] T. Koutzarova, S. Kolev, I. Nedkov (etal), J. Supercond Nov Magn DOI 10.1007/s10948-011-1232-3.
[24] J. Singhal, S. K. Singh, K.Barthwal, J. Chandra, of Solid State Chemistry, Vol. 178, No. 10, 2005, 3183-89.
[25] G. K. Joshi, S. A. Deshpande, A. Y. Khot, S. R. Sawant, Ind. J. Phys. A 61 (1987) 241.

Licensed Under Creative Commons Attribution CC BY